



# The Dynamic Behaviors of Photosynthesis during Non-Motile Cell Germination in *Haematococcus pluvialis*

Qianqian Li <sup>1,\*</sup> , Bo Li <sup>2,3</sup> and Junmin Li <sup>2,3</sup> 

<sup>1</sup> Key Laboratory of South China Agricultural Plant Molecular Analysis and Genetic Improvement & Guangdong Provincial Key Laboratory of Applied Botany, South China Botanical Garden, Chinese Academy of Sciences, Guangzhou 510650, China

<sup>2</sup> State Key Laboratory of Tropical Oceanography, Guangdong Provincial Observation and Research Station for Coastal Upwelling Ecosystem, South China Sea Institute of Oceanology, Chinese Academy of Sciences, Guangzhou 511458, China; libo@scsio.ac.cn (B.L.); jli@scsio.ac.cn (J.L.)

<sup>3</sup> Southern Marine Science and Engineering Guangdong Laboratory (Guangzhou), Guangzhou 511458, China

\* Correspondence: liqianqian@scbg.ac.cn; Tel.: +86-20-37252711

**Abstract:** *Haematococcus pluvialis* undergoes a three-phase process during the process of germination: first, repeated mitotic events; next, cytokinesis to form the zoospore; and finally, a fast release of motile cells. Physiological properties were measured using chlorophyll *a* fluorescence (OJIP) transient. The most obvious increase in K-value and L-value appeared at 17 h, suggesting that oxygen-evolving complex damage and lower energetic connectivity of the photosystem II units of the mother non-motile cell occurred. Compared to phase I, the values of the maximum quantum yield of PSII photochemistry ( $F_v/F_m$ ) and  $PI_{ABS}$  increased significantly in phases II and III, suggesting that photosynthetic photochemical activity was greatly up-regulated during cytokinesis to form zoospores and the fast release of motile cells. Moreover, the significant increase in the K-band at 17 h and 22 h indicates that the PSII donor side was the limiting factor during the initial period of germination. All these results suggest that the cellular photosynthetic activity continues to strengthen during cytokinesis to form the zoospore and the fast release of motile cells, and it was postulated to meet the demands for sporangium swelling and new organelle formation.

**Keywords:** *Haematococcus pluvialis*; non-motile cell; motile cell; germination; chlorophyll *a* fluorescence transient; photosynthetic behavior



**Citation:** Li, Q.; Li, B.; Li, J. The Dynamic Behaviors of Photosynthesis during Non-Motile Cell Germination in *Haematococcus pluvialis*. *Water* **2022**, *14*, 1280. <https://doi.org/10.3390/w14081280>

Academic Editor: Anas Ghadouani

Received: 8 March 2022

Accepted: 13 April 2022

Published: 15 April 2022

**Publisher's Note:** MDPI stays neutral with regard to jurisdictional claims in published maps and institutional affiliations.



**Copyright:** © 2022 by the authors. Licensee MDPI, Basel, Switzerland. This article is an open access article distributed under the terms and conditions of the Creative Commons Attribution (CC BY) license (<https://creativecommons.org/licenses/by/4.0/>).

## 1. Introduction

*Haematococcus pluvialis* is of great interest because it may amass a considerable amount of the antioxidant astaxanthin [1,2]. In previous studies, the cell cycles and proliferation patterns of *Haematococcus pluvialis* had been described based on repeated microscopic observation [3]. The germination of non-motile cells into motile cells is critical for cell recovery from resting spores during its complex life cycle. Three phases were identified to obtain deeper insights into the metabolic changes taking place during this process. The first phase (phase I, 0–12 h) consists of repeated mitotic events, in which the cell begins to expand. Then, the cell initiates cytokinesis to form the zoospores within the mother non-motile cell and prepares for their release (phase II, 12–17 h). After 17 h of induction, the cell wall of the mother non-motile cell ruptures, and the new motile cells are released (phase III, 17–22 h) [4]. Water uptake is the first step for the initiation of red non-motile cell germination, followed by metabolic recovery and the formation of sporangia, and finally the rupture of the sporangial walls, which results in the release of a new generation of zoospores. Germination was associated with chlorophyll and protein synthesis, as well as carotenoid degradation, in addition to the drastic changes in cell shape [5,6]. The ratio of carotenoid/chlorophyll continuously decreased from  $7.0 \pm 0.7$  (non-motile cells) to  $0.3 \pm 0.1$  (motile cells) [7]. From the evidence, we speculated that photosynthesis activity

gradually recovered during non-motile cell germination, which is still being debated. Meanwhile, how about the rate of recovery of various steps of photosynthesis? Which one is the rate-limiting step of photosynthesis? However, related research on this area remains sparse. Therefore, studying the dynamic behaviors of photosynthesis during non-motile cell germination in *Haematococcus pluvialis* is of substantial significance for exploring the metabolic changes taking place during this process. Chlorophyll *a* fluorescence OJIP transient (OJIP transient) is a useful method for analyzing and screening photosynthetic samples [8]. The OJIP transient, which is characterized by O, J, I, and P steps, is especially useful in the study of PSII activity in plants, algae, and cyanobacteria [9,10]. Combining the corresponding physiological property changes and then analyzing the coordination with photosynthesis-related unigenes at the transcript level would be helpful to further understand the algal metabolism regulatory mechanisms during the process of *H. pluvialis* non-motile cell germination. Based on the above, qualitative and quantitative analyses of PSII behavior changes were emphasized using the OJIP transient combined with JIP-test. Meanwhile, the respiration rate and total O<sub>2</sub> evolution rate were also analyzed to elucidate the regulatory mechanism of the photosystem during *H. pluvialis* non-motile cell germination.

## 2. Materials and Methods

### 2.1. Culture Conditions

An algal culture strain of *H. pluvialis* (strain number: H7) was obtained from the Yunnan Alphy Biotech Co., Ltd., Chuxiong, Ziwu Village, Yunnan province, China (24°89' N, 101°5' E). For observation of the life cycle, the cells were cultured in MCM medium under natural conditions with a 14:10 h light–dark cycle. The cultures were irradiated with a fluorescent lamp at approximately 100  $\mu\text{mol photons m}^{-2} \text{s}^{-1}$  to stimulate the formation of thick-walled non-motile cells. These four *Haematococcus pluvialis* samples (0, 12, 17, and 22 h) used in this study were collected and processed as described in our 2019 paper (Figure 1) [4].

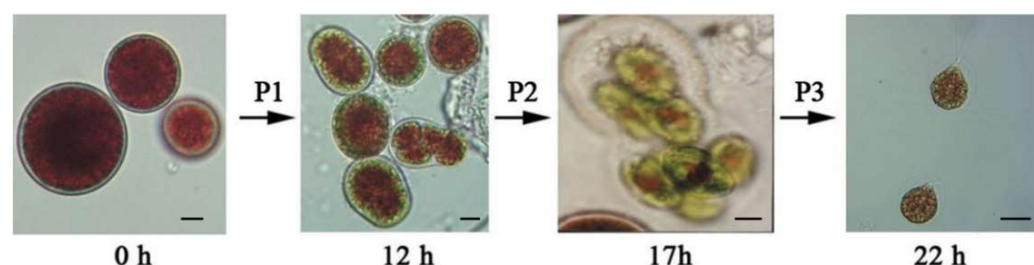


**Figure 1.** Light microscopic images of four sampling points during *H. pluvialis* non-motile cell germination. 0 h, non-motile cells; 12 h, repeated mitotic events within the mother non-motile cell; 17 h, cytokinesis to form the zoospores within the mother non-motile cell; 22 h, cell wall of the mother non-motile cell ruptures and the new motile cells are released. P1, P2, and P3 are short for phase I, phase II, and phase III, respectively. The length of each bar represents 10  $\mu\text{m}$ .

### 2.2. Physiological Measurements

Chlorophyll (Chl) *a* fluorescence (OJIP) transients were monitored using a Handy PEA fluorimeter (Hansatech, Pentney, UK). All measurements were carried out with samples that had been dark-adapted for 10 min. The JIP-test was used to examine the OJIP transients [11]. Saturating red light at 3000  $\mu\text{mol photons m}^{-2} \text{s}^{-1}$  was produced by an array of light-emitting diodes (LED, peak 650 nm). The chlorophyll *a* fluorescence transients were obtained using 1 s saturating red light and analyzed with the OJIP-test. The relevant parameters and their significance involved in the experiment are shown in Table 1. The total photosynthetic O<sub>2</sub> evolution rate and respiration rate were measured using a Clark-type O<sub>2</sub> electrode (Hansatech, Norfolk, UK) at 20 °C and 100  $\mu\text{mol/m}^2/\text{s}$  PFD according to Yu et al. [12]. The initial cell density was about  $1.0 \times 10^6$  cells  $\text{mL}^{-1}$  and NaHCO<sub>3</sub> (1 mM)

was the acceptor during the measurements of  $O_2$  evolution. The results were analyzed using ANOVA multiple  $t$ -tests ( $p < 0.05$ ) to determine the statistical significance between experimental groups. Detection and enrichment of DEGs related to energy metabolism were carried out according to our 2019 paper, based on the corresponding transcriptomic data [4].

**Table 1.** Definitions and explanations of selected JIP-test parameters derived from the chlorophyll  $a$  fluorescence induction curve.

Parameters	Description
$V_J$	Relative variable fluorescence at the J-step.
$F_V/F_M$	Maximum quantum yield of PSII photochemistry.
$PI_{ABS}$	Performance index on absorption basis.
$RC/ABS$	Efficiency of reaction centers
$\phi Po/(1-\phi Po)$	Light energy absorption efficiency
$\psi o/(1-\psi o)$	Acceptance efficiency of electron acceptors
$ABS/RC$	Absorption flux (for PSII antenna chlorophylls) per reaction center (RC)
$TR_O/RC$	Trapped energy flux (leading to $Q_A$ reduction) per reaction center RC
$ET_O/RC$	Electron transport flux (further than $Q_A^-$ ) per PSII RC (at $t = 0$ )
$DI_O/RC$	Dissipated energy flux per reaction center RC (at $t = 0$ )

### 3. Results and Discussion

#### 3.1. Photosynthesis and Respiration

During the first 12 h of incubation, *H. pluvialis* maintained a relatively high respiratory rate (phase I, repeated mitotic events), compared to phase II (cytokinesis to form the zoospore). The total  $O_2$  evolution rate increased dramatically in the following 12–17 h of incubation (phase II, cytokinesis to form the zoospore). Meanwhile, the change of net photosynthetic  $O_2$  evolution rate was synchronized with the change of total photosynthetic  $O_2$  evolution rate, but a slower rate due to an increase in respiratory rate during 17–22 h (phase III, a fast release of motile cells) (Figure 2B). The carbon skeleton and energy for the non-motile cell germination were mostly derived from photosynthesis and respiration. It was suggested that red non-motile cells accumulate higher levels of carbohydrates and oil droplets than green vegetative motile cells [1,13]. Non-motile cell germination can be induced even under low light or in the dark [7,14,15]. All of the findings indicate that respiration plays an important role in the non-motile cell germination of *H. pluvialis*.

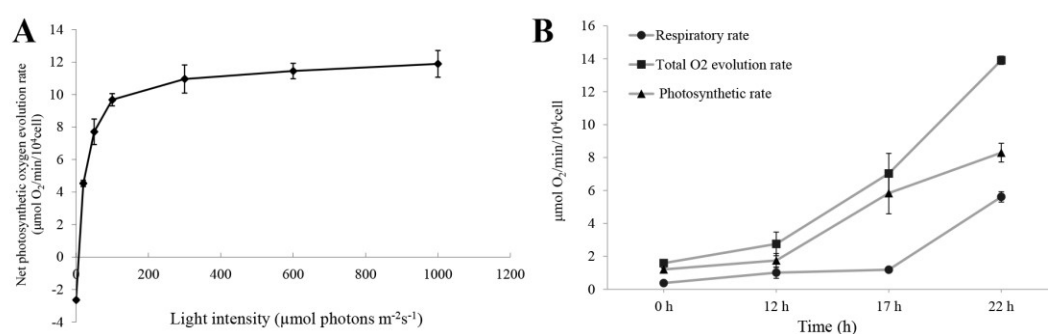


**Figure 2.** (A) Light response curve for net photosynthetic  $O_2$  evolution rate of *H. pluvialis* cells. (B) The respiration rate, net photosynthetic  $O_2$  evolution rate, and total photosynthetic  $O_2$  evolution rate during *H. pluvialis* non-motile cell germination. Mean  $\pm$  SE of five replicates were presented.

### 3.2. Chlorophyll *a* Fluorescence Intensity Curve (OJIP)

The fluorescence transients of these four samples were presented in Figure 3. *H. pluvialis* at 17 h and 22 h showed the typical OJIP chlorophyll fluorescence transient. In contrast, samples of 0 h and 12 h showed an obvious up-regulation at the J step and down-regulation at the I step, respectively. The shape and intensity of OJIP transients at 0 h and 12 h showed distinctive differences at 17 h and 22 h (Figure 3A), implying that photosystem (PS) II behaviors were altered during *H. pluvialis* non-motile cell germination. To clarify the detailed alternations of PSII behaviors during this process, the variations in the phases of O-J, O-K, and O-I in the relative variable fluorescence kinetics were examined by normalizing the OJIP transients (Figure 3B–D). Lazar et al., demonstrated that the appearance of the K step could be related to many functional and structural moments in PSII, and the inhibition of OEC is one of the most important reasons [16]. In this study, the most obvious increase in the K-value and  $V_J$  values appeared at 17 h, followed by 22 h, 12 h, and 0 h (Figure 3B). This meant that the acceptor side and reaction centers of PSII recover more quickly at 17 h, in contrast to the donor side of PSII. Therefore, the increase in K-band was mainly caused by the inhibition of the donor side of PSII. Meanwhile, the so-called L-band was also found and was greatly increased at 17 h (Figure 3C). It is remarkably, however, the photosynthetic electron transport was still sufficient to support photosynthesis, even though the donor side was limited. Carbon assimilation might be the limiting factor instead of photosynthetic electron transport. The decreased energetic connectivity of the PSII units was suggested by the higher L band, which meant that the PSII units were less grouped or less energy was being exchanged between the independent PSII units [17]. All these results suggest that the 17 h sample had poor utilization of the excitation energy. Figure 3D was plotted to show the amplitude of the I-P phase. It was found that the amplitudes of the I-P phase decreased at 12 h first, followed by a further decrease at 17 h, then an obvious increase was observed at 22 h. These results indicated the number of final electron acceptors at PSI experienced a large decrease during 0–17 h, and the maximal accumulation of end electrons at PSI occurred at 17 h. The accumulation of excess electrons may lead to cell damage and generate ROS [11].

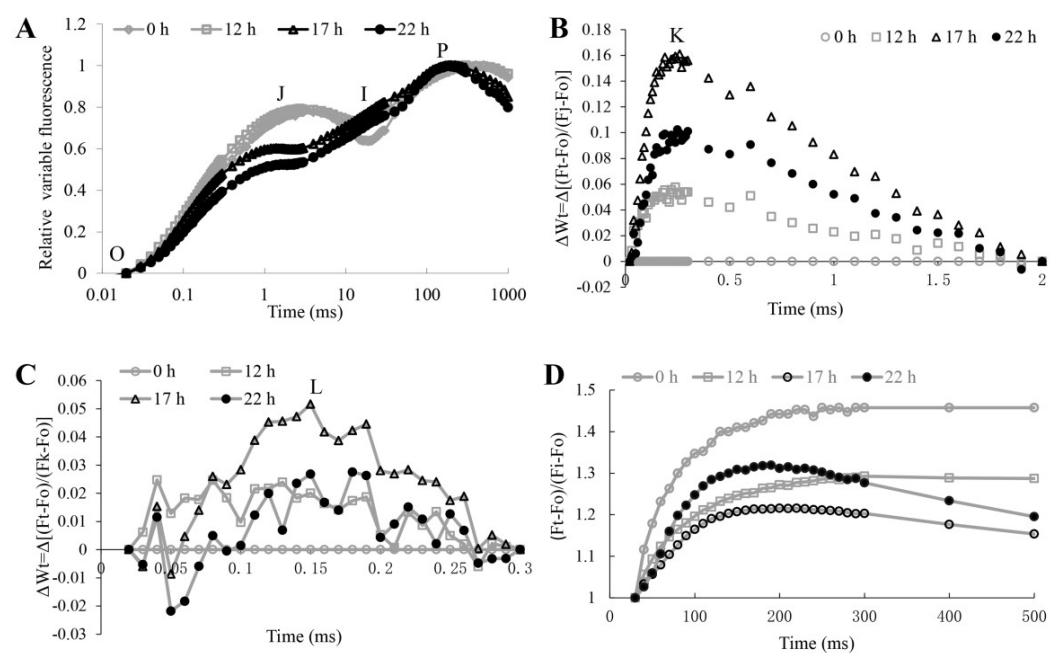


**Figure 3.** (A) During *H. pluvialis* non-motile cell germination, changes in chlorophyll *a* fluorescence transient (OJIP) are displayed on a logarithmic time scale (0 h, 12 h, 17 h, and 22 h). Curves are expressed as relative variable fluorescence intensity ( $V_t$ ), i.e., double normalized at the  $F_0$  and  $F_P$  points ( $V_t = (F_t - F_0)/(F_P - F_0)$ ). (B,C)  $\Delta W_t$  transient kinetics, i.e., the values double normalized at

the  $F_O$  and  $F_J$  points (B) and the  $F_O$  and  $F_K$  points (C), during *H. pluvialis* non-motile cell germination (12 h, 17 h, and 22 h), after subtraction of the control (0 h), given on a linear time scale. (D) Upper part of chlorophyll (Chl) fluorescence transient from I to P, after double normalization between the  $F_O$  and  $F_I$  points. Data from four samples were collected during the non-motile cell germination of *H. pluvialis* (0 h, 12 h, 17 h, and 22 h). Note that the starting point on the x-axis is 1 and the O-J-I part of the transient is omitted. Each curve represents a mean of 10 independent transients ( $n = 10$ ).

Apart from qualitative analysis, quantitative analysis using the JIP-test was also performed to elucidate the change in PSII behaviors. The value of  $F_V/F_M$  largely reflects the maximum quantum yield of PSII photochemistry. In addition, the  $PI_{ABS}$  is more sensitive to changes in photosynthetic activity than the  $F_V/F_M$  [10], and it is closely related to energy conservation and behaviors of the photosynthetic apparatuses. In this study, the values of  $F_V/F_M$  and  $PI_{ABS}$  increased significantly at 17 h and 22 h. This indicated that PSII photochemical efficiency was increased, and the photosystem experienced an increase in energy conservation and a considerable activation of energy trapping at 17 h and 22 h. These results suggested that photosynthetic efficiency increased and the photosynthetic apparatuses in *H. pluvialis* were opened to a certain extent along with non-motile germination (17 h and 22 h). Meanwhile, the high value of  $V_J$  reflects the high level of closures of RCs. In this study, the higher  $V_J$  values at 0 h and 12 h indicated that the closed RCs of PSII increased during phase I (cell begins to expand). As germination occurred, *H. pluvialis* showed a significant decrease in 17 h and 22 h in the  $V_J$  value compared with 0 h and 12 h. This result suggested that algal cells at 17 h and 22 h had an increase in open RCs, which would raise the possibility of electron transferred from  $Q_A$  to  $Q_B$  and further cause a lower fractional rate of  $Q_A$  reduction. These results indicated that the open RCs of PSII increased during phases II and III. Additionally, the Mo value decreased as germination continued (17 h), indicating that *H. pluvialis* had a lower fractional rate of  $Q_A$  reduction (namely, a lower energy flux from the antenna to PSII RCs), and the electron transfer from  $Q_A$  to  $Q_B$  was activated to a certain extent during zoospore formation of cytokinesis (phase II). The appearance continued until 22 h with a smaller range.

At 17 h and 22 h, *H. pluvialis* showed a considerable rise in  $\psi_o$  values (0.397 and 0.450, respectively, whereas 0.237 at 0 h), indicating that electron transport in the PSII electron transport chain was positively influenced. Values of  $\phi_{Eo}$  were congruent with values of  $\psi_o$  ( $\phi_{Eo}$  values were 0.283 and 0.363 at 17 h and 22 h, respectively, while the control was 0.008), suggesting that the electron transport quantum yield increased with the development of *H. pluvialis* non-motile cell germination process, and the microalgae maintained a high capacity for the electron transport during phase III. The light energy absorption efficiency ( $\phi_{Po}/(1-\phi_{Po})$ ) was also greatly increased at 17 h and 22 h. However, compared with 0 h, the efficiency of RCs (RC/ABS) and the accepting efficiency of electron acceptors ( $\psi_o/(1-\psi_o)$ ) showed no significant increase in 17 h and 22 h.

The ABS/RC ratio is calculated by dividing the total number of photons absorbed by Chl molecules in all RCs divided by the total number of open RCs. Yusuf et al. (2000) have deduced that the inactivation of a fraction of RCs or the increase in functional antenna would lead to an increase in ABS/RC [17]. Accordingly, the decrease in ABS/RC ratio of this study, indicates that (i) a fraction of the RCs in algal cells were activated, or (ii) the functional antenna, i.e., the antenna that feeds excitation energy to open RCs, decreased in size (Table 2). Similar to the phenomenon of the aerial microalga *Trentepohlia jolithus* [18], the slight increase in  $TR_O/RC$  suggested that the first case was probably the reason for the ABS/RC decreases.  $ET_O/RC$  denotes the reoxidation of reduced  $Q_A$  via electron transport in an open RC. At 0 h and 12 h,  $ET_O/RC$  ratio was lower than that at 17 h and 22 h, which suggested that the reoxidation of  $Q_A$  was blocked and  $Q_B$  could not obtain electrons from  $Q_A$ . This situation was improved until 17 h. Meanwhile, the ratio of  $DI_O/RC$ , which represents the total dissipation of untrapped excitation energy from all RCs with respect to the number of open RCs [19], showed the same pattern as ABS/RC. These results suggested that open RCs decreased heat dissipation as energy transferred to other systems to avoid damage that would be caused by the excess energy. Additionally, more remarkable, high



astaxanthin content at 0 h and 12 h might be the reason for the high ratio of  $DI_O/RC$ , resulting in photosystem protection against damage, at least to a certain extent [20].

**Table 2.** Statistical comparison of parameters obtained from the JIP-test of four samples.

Parameters	0 h	12 h	17 h	22 h
$V_J$	$0.763 \pm 0.052^b$	$0.792 \pm 0.105^b$	$0.603 \pm 0.010^a$	$0.550 \pm 0.067^a$
$F_V/F_M$	$0.356 \pm 0.023^a$	$0.504 \pm 0.078^b$	$0.712 \pm 0.008^c$	$0.810 \pm 0.035^d$
$PI_{ABS}$	$0.024 \pm 0.015^a$	$0.060 \pm 0.054^a$	$0.361 \pm 0.035^b$	$0.996 \pm 0.304^c$
$RC/ABS$	$0.138 \pm 0.050^a$	$0.181 \pm 0.021^b$	$0.221 \pm 0.005^c$	$0.271 \pm 0.023^d$
$\varphi_{Po}/(1-\varphi_{Po})$	$0.553 \pm 0.130^a$	$1.041 \pm 0.320^a$	$2.474 \pm 0.097^b$	$4.423 \pm 1.097^c$
$\psi_o/(1-\psi_o)$	$0.311 \pm 0.090^a$	$0.274 \pm 0.069^a$	$0.659 \pm 0.026^b$	$0.840 \pm 0.251^b$
$ABS/RC$	$7.253 \pm 0.380^d$	$5.565 \pm 0.645^c$	$4.530 \pm 0.097^b$	$3.706 \pm 0.240^a$
$TR_O/RC$	$2.582 \pm 0.290^a$	$2.780 \pm 0.108^{ab}$	$3.225 \pm 0.039^c$	$2.998 \pm 0.127^{bc}$
$ET_O/RC$	$0.614 \pm 0.130^a$	$0.585 \pm 0.314^a$	$1.281 \pm 0.022^b$	$1.338 \pm 0.112^b$
$DI_O/RC$	$4.668 \pm 0.410^d$	$2.786 \pm 0.754^c$	$1.306 \pm 0.063^b$	$0.708 \pm 0.175^a$

Note: Means  $\pm$  SD relative to the respective controls (0 h), of 10 replicates ( $n = 10$ ) are presented. Different letters indicate significant differences among different samples during *H. pluvialis* non-motile cell germination ( $p < 0.05$ ).

All these results suggest that *H. pluvialis* cells in phases I and II had poor utilization of excitation energy, which would cause an imbalance between photosynthetic light absorption and energy utilization under high light, leading to ROS generation and cell damage. Therefore, low light or darkness should be applied to prevent photodamage during phases I and II of cell germination, in this situation, respiration could supply carbon skeleton and energy for the non-motile cell germination. During phase III of cell germination, photosynthetic efficiency increased and the photosynthetic apparatuses were opened to a certain extent. In this situation, high light can be applied to induce photomorphogenesis, such as chlorophyll synthesis in *H. pluvialis* cells.

### 3.3. Expression of Energy Metabolism-Related Unigenes at the Transcript Level

Plant metabolism underpins many traits of ecological and agronomic importance. In previous studies, mRNA expression of these four-time points during *H. pluvialis* non-motile cell germination, especially for carbohydrate metabolism and lipid metabolism, was examined using comparative transcriptome data [4]. To better understand the metabolic changes that occur during the transition from non-motile cells to motile cells, differential expression analysis of energy metabolism-related unigenes was illustrated in this study (Supplementary Materials Table S1).

With the enlargement of red non-motile cells (phase I), few DEGs were present in energy metabolism (Figure 4). This was consistent with the conclusion that resting cells, with fragmented thylakoid membranes, maintained moderate photosynthesis [21]. The largest amounts of DEGs were present in phase II (Figure 4). The enhanced PsaH and PetF expression levels consequently improved the capacity of photosystem I [22] and facilitated biomass generation by transferring extra electrons generated from photosynthesis to enzymes involved in biomass formation [23]. In phase III, the down-regulation of PsbP and PetF weaken photosynthetic activity after the completion of material and energy preparation. The differential expression of Lhca, which were up-regulated in phase II and then down-regulated sharply to the original level during phase III, seemed to be consistent with the utilization of light energy [24]. The above results were consistent with the PSII activity change during *H. pluvialis* non-motile cell germination. The specific-phase (I and III) down-regulation of two F-type  $H^+$ -transporting ATPase subunits, which are located on the inner membrane of mitochondria and thylakoid membrane of chloroplasts, indicated less ATP synthesis [25]. Meanwhile, overexpression of four V-type  $H^+$ -transporting ATPase subunits

in phase II, which were basically located on vacuoles, would provide more energy for ion transporters, cause vacuole acidification and cause sporangium swelling [26]. The carbon flux for the synthesis of cell macromolecules was mostly in equilibrium with the energy flux provided by photosynthesis [27]. This suggested that light energy absorption would exert a driving force for the release of motile cells. Meanwhile, up-regulation of unigenes related to glycolysis, TCA cycle, and fatty acid synthesis in phase II was also observed in the previous study, which was consistent with the conclusion that respiration played an important role in non-motile cell germination of *H. pluvialis*. In addition to carbohydrate metabolism and lipid metabolism, the algal cells probably maintained stronger energy metabolic activity in phase II.

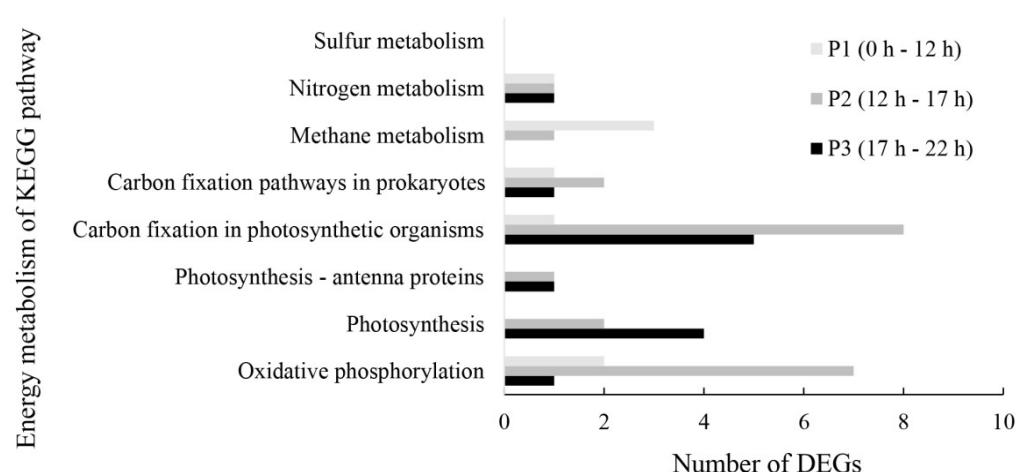


**Figure 4.** Number of differential expression genes involved in energy metabolism after pair-wise comparison.

#### 4. Conclusions

The cell development stages of unicellular algae play an important role in the regulation mechanism of the photosystem. At the beginning of non-motile cell germination, the catabolism of stored reserves of starch and oil accumulated during non-motile cell formation supports cell expansion and chloroplast development until photoautotrophic growth can be resumed. Compared to 0 h and 12 h, the algae showed higher photosynthetic photochemical activity at 17 h and 22 h. In phase I, reoxidation of  $Q_A$  was partly blocked, the electron transport from  $Q_A$  to  $Q_B$  is impaired. PSII RCs were still closed, and closed RCs were able to dissipate excess excitation energy as heat. In phase II, the PSII RCs of *H. pluvialis* were opened and light absorption and photosynthetic electron transport became much more efficient. This will contribute to the increase in photosynthetic efficiency. In phase III, the open RCs decreased heat dissipation and electron transfer became more efficient. In addition, the uncoupling of OEC (K-peak appeared) at 17 h and 22 h might be due to the cell division of this phase. Meanwhile, accompanying the increase in photosynthetic photochemical activity, many metabolism related-unigenes were also greatly up-regulated during phases II and III. The changes in gene expression and photosynthetic characteristics were likely to meet the demands for sporangium swelling and new organelle formation, such as vacuoles, flagella, and chloroplasts. This study will provide valuable and reliable insights into the photosynthetic process involved in the non-motile cell germination of *Haematococcus pluvialis* and provide a technical reference to the development of its large-scale cultivation.

**Supplementary Materials:** The following are available online at <https://www.mdpi.com/article/10.3390/w14081280/s1>, Table S1: Differentially expressed gene statistics among energy metabolism.

**Author Contributions:** Conceptualization, Q.L.; methodology, Q.L.; validation, B.L. and Q.L.; data curation, B.L. and Q.L.; review and editing, Q.L., B.L. and J.L.; funding acquisition, Q.L., B.L. and J.L. All authors have read and agreed to the published version of the manuscript.

**Funding:** This research was funded by the Natural Science Foundation of Guangdong Province (2019A1515012066), the Science and Technology Program of Guangzhou (202102020839), the Key Special Project for Introduced Talents Team of Southern Marine Science and Engineering Guangdong Laboratory (Guangzhou) (GML2019ZD0303), the Science and Technology Projects of Guangdong Province (2021B1212050023), and the Strategic Priority Research Program of the Chinese Academy of Sciences (XDA13030304).

**Institutional Review Board Statement:** Not applicable.

**Informed Consent Statement:** Not applicable.

**Data Availability Statement:** No data, models, or code were generated or used during the study.

**Acknowledgments:** Special thanks to Yongbiao Lin and Heshan National Field Research Station of Forest Ecosystem of South China Sea Institute of Oceanology, Chinese Academy of Sciences for their provisions on assets and services.

**Conflicts of Interest:** The authors state that this research is free of conflicts of interest.

## Abbreviations

PSI: Photosystem I  
 PSII: Photosystem II  
 Chl: chlorophyll  
 OEC: oxygen-evolving complex  
 ROS: reactive oxygen species  
 DEG: differentially expressed genes  
 PsaH: photosystem I subunit VI  
 PsbP: photosystem II oxygen-evolving enhancer protein 2  
 PetF: ferredoxin  
 TCA cycle: tricarboxylic cycle  
 Lhc: light harvesting complexes

## References

- Shah, M.M.; Liang, Y.; Cheng, J.J.; Daroch, M. Astaxanthin-producing green microalga *Haematococcus pluvialis*: From Single Cell to High Value Commercial Products. *Front. Plant Sci.* **2016**, *7*, 531. [\[CrossRef\]](#)
- Takaichi, S. Carotenoids in Algae: Distributions, biosyntheses and functions. *Mar. Drugs* **2011**, *9*, 1101–1118. [\[CrossRef\]](#)
- Zhang, C.H.; Liu, J.G.; Zhang, L.T. Cell cycles and proliferation patterns in *Haematococcus pluvialis*. *Chin. J. Oceanol. Limn.* **2017**, *35*, 1205–1211. [\[CrossRef\]](#)
- Li, Q.Q.; Zhang, L.T.; Liu, J.G. Examination of carbohydrate and lipid metabolic changes during *Haematococcus pluvialis* non-motile cell germination using transcriptome analysis. *J. Appl. Phycol.* **2019**, *31*, 145–156. [\[CrossRef\]](#)
- Mesquita, J.F.; Santos, M.F. Ultrastructural study of *Haematococcus lacustris* (Girod.) Rostafinski (Volvocales). II. Mitosis and cytokinesis. *Cytologia* **1984**, *49*, 229–241. [\[CrossRef\]](#)
- Liu, J.G.; Zhang, J.P. Photosynthetic and respiration rate of *Haematococcus pluvialis*. *Oceanol. Limnol. Sin.* **2000**, *31*, 6.
- Kobayashi, M.; Kurimura, Y.; Kakizono, T.; Nishio, N.; Tsuji, Y. Morphological changes in the life cycle of the green alga *Haematococcus pluvialis*. *J. Ferment. Bioeng.* **1997**, *84*, 94–97. [\[CrossRef\]](#)
- Strasser, R.J. Analysis of the Fluorescence Transient. In *Chlorophyll a Fluorescence*; Springer: Dordrecht, The Netherlands, 2004.
- Jimenez-Francisco, B.; Stirbet, A.; Aguado-Santacruz, G.A.; Campos, H.; Conde-Martinez, F.V.; Padilla-Chacon, D.; Trejo, C.; Bernacchi, C.J.; Govindjee, G. A comparative chlorophyll a fluorescence study on isolated cells and intact leaves of *Bouteloua gracilis* (blue grama grass). *Photosynthetica* **2020**, *58*, 262–274. [\[CrossRef\]](#)
- Stirbet, A.; Lazar, D.; Kromdijk, J.; Govindjee. Chlorophyll a fluorescence induction: Can just a one-second measurement be used to quantify abiotic stress responses? *Photosynthetica* **2018**, *56*, 86–104. [\[CrossRef\]](#)
- Li, H.; Liu, J.G.; Zhang, L.T.; Pang, T. Effects of low temperature stress on the antioxidant system and photosynthetic apparatus of *Kappaphycus alvarezii* (Rhodophyta, Solieriaceae). *Mar. Biol. Res.* **2016**, *12*, 1064–1077. [\[CrossRef\]](#)
- Yu, W.J.; Zhang, L.T.; Zhao, J.; Liu, J.G. Exogenous sodium fumarate enhances astaxanthin accumulation in *Haematococcus pluvialis* by enhancing the respiratory metabolic pathway. *Bioresour. Technol.* **2021**, *341*, 125788. [\[CrossRef\]](#)



13. Hagen, C.; Siegmund, S.; Braune, W. Ultrastructural and chemical changes in the cell wall of *Haematococcus pluvialis* (Volvocales, Chlorophyta) during aplanospore formation. *Eur. J. Phycol.* **2002**, *37*, 217–226. [\[CrossRef\]](#)
14. Lee, Y.K.; Ding, S.Y. Cell-Cycle and Accumulation of Astaxanthin in *Haematococcus-Lacustris* (Chlorophyta). *J. Phycol.* **1994**, *30*, 445–449. [\[CrossRef\]](#)
15. Wayama, M.; Ota, S.; Matsuura, H.; Nango, N.; Hirata, A.; Kawano, S. Three-dimensional ultrastructural study of oil and astaxanthin accumulation during encystment in the green alga *Haematococcus pluvialis*. *PLoS ONE* **2013**, *8*, e53618. [\[CrossRef\]](#)
16. Lazar, D. Chlorophyll a fluorescence induction. *BBA Bioenerg.* **1999**, *1412*, 1–28. [\[CrossRef\]](#)
17. Yusuf, M.A.; Kumar, D.; Rajwanshi, R.; Strasser, R.J.; Tsimilli-Michael, M.; Govindjee; Sarin, N.B. Overexpression of gamma-tocopherol methyl transferase gene in transgenic *Brassica juncea* plants alleviates abiotic stress: Physiological and chlorophyll a fluorescence measurements. *BBA Bioenerg.* **2010**, *1797*, 1428–1438. [\[CrossRef\]](#)
18. Zhang, L.; Li, Y.; Liu, J. Complete inactivation of photosynthetic activity during desiccation and rapid recovery by rehydration in the aerial microalga *Trentepohlia jolithus*. *Plant Biol.* **2016**, *18*, 1058–1061. [\[CrossRef\]](#)
19. Mathur, S.; Jajoo, A.; Mehta, P.; Bharti, S. Analysis of elevated temperature-induced inhibition of photosystem II using chlorophyll a fluorescence induction kinetics in wheat leaves (*Triticum aestivum*). *Plant Biol.* **2011**, *13*, 1–6. [\[CrossRef\]](#)
20. Li, Y.; Sommerfeld, M.; Chen, F.; Hu, Q. Consumption of oxygen by astaxanthin biosynthesis: A protective mechanism against oxidative stress in *Haematococcus pluvialis* (Chlorophyceae). *J. Plant Physiol.* **2008**, *165*, 1783–1797. [\[CrossRef\]](#)
21. Gu, W.H.; Xie, X.J.; Gao, S.; Zhou, W.; Pan, G.H.; Wang, G.C. Comparison of different cells of *Haematococcus pluvialis* reveals an extensive acclimation mechanism during its aging process: From a perspective of photosynthesis. *PLoS ONE* **2013**, *8*, e67028. [\[CrossRef\]](#)
22. Song, A.; Li, P.; Fan, F.L.; Li, Z.J.; Liang, Y.C. The effect of silicon on photosynthesis and expression of its relevant genes in rice (*Oryza sativa* L.) under High-Zinc Stress. *PLoS ONE* **2014**, *9*, e113782. [\[CrossRef\]](#)
23. Lin, Y.H.; Pan, K.Y.; Hung, C.H.; Huang, H.E.; Chen, C.L.; Feng, T.Y.; Huang, L.F. Overexpression of ferredoxin, PETF, enhances tolerance to heat stress in *Chlamydomonas reinhardtii*. *Int. J. Mol. Sci.* **2013**, *14*, 20913–20929. [\[CrossRef\]](#)
24. Caffarri, S.; Tibiletti, T.; Jennings, R.C.; Santabarbara, S. A Comparison between plant photosystem i and photosystem ii architecture and functioning. *Curr. Protein Pept. Sci.* **2014**, *15*, 296–331. [\[CrossRef\]](#)
25. Graber, P.; Labahn, A. Proton transport-coupled unisite catalysis by the H<sup>+</sup>-atpase from Chloroplasts. *J. Bioenerg. Biomembr.* **1992**, *24*, 493–497. [\[CrossRef\]](#)
26. Zhang, X.H.; Li, B.; Hu, Y.G.; Chen, L.; Min, D.H. The Wheat E Subunit of V-type H<sup>+</sup>-ATPase is involved in the plant response to osmotic stress. *Int. J. Mol. Sci.* **2014**, *15*, 16196–16210. [\[CrossRef\]](#)
27. Wagner, H.; Jakob, T.; Fanesi, A.; Wilhelm, C. Towards an understanding of the molecular regulation of carbon allocation in diatoms: The interaction of energy and carbon allocation. *Philos. Trans. R. Soc. B Biol. Sci.* **2017**, *372*, 20160410. [\[CrossRef\]](#)